Supporting Information

Inverse sandwich complexes of $B_7M_2^-$, B_8M_2, and $B_9M_2^+$ (M=Zr, Hf): The nonclassical M-M bonds embedded in monocyclic boron rings

Zhong-hua Cui,*[ad] Chen Chen,[a] Qing Wang,[c] Lili Zhao,*[c] Meng-hui Wang,[a] and Yi-hong Ding*[b]

[a]*Institute of Atomic and Molecular Physics, Jilin University, Changchun, China*
E-mail: zcui@jlu.edu.cn
[b]*Institute of Theoretical Chemistry, Jilin University, Changchun, China*
E-mail: yhdd@jlu.edu.cn
[c]*Institute of Advanced Synthesis, School of Chemistry and Molecular Engineering, Nanjing Tech University, Nanjing, China*
E-mail: ias_llzhao@njtech.edu.cn
[d]*Beijing National Laboratory for Molecular Sciences*

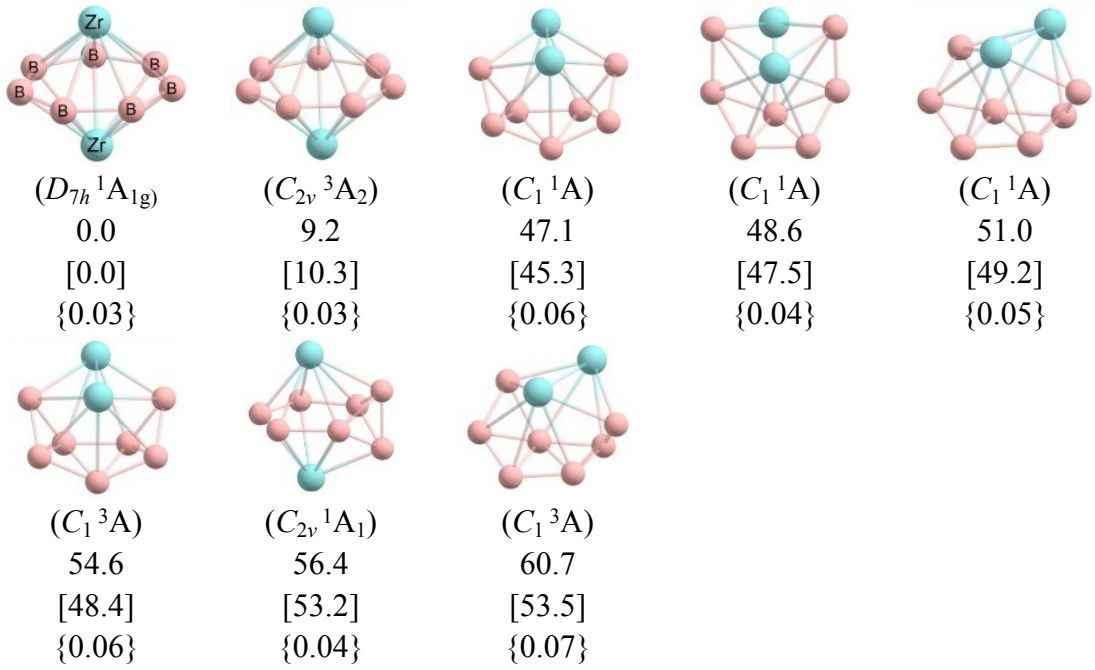

(D_{7h} $^1A_{1g}$)	(C_{2v} $^3A_2$)	(C_1 ^1A)	(C_1 ^1A)	(C_1 ^1A)
0.0	9.2	47.1	48.6	51.0
[0.0]	[10.3]	[45.3]	[47.5]	[49.2]
{0.03}	{0.03}	{0.06}	{0.04}	{0.05}

(C_1 ^3A)	(C_{2v} $^1A_1$)	(C_1 ^3A)
54.6	56.4	60.7
[48.4]	[53.2]	[53.5]
{0.06}	{0.04}	{0.07}

Figure S1. Optimized structures of $B_7Zr_2^-$ at the PBE0/Def2-TZVPP level. The relative energy in kcal/mol computed at the single-point CCSD(T)/Def2-TZVPP//PBE0/Def2-TZVPP and PBE0/Def2-TZVPP (in square brackets) level with zero-point corrections of PBE0/Def2-TZVPP. T1 diagnostic, point group and spectroscopic states were given in curly brace and parenthesis, respectively.

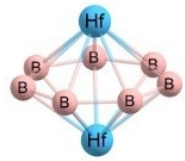

(D_{7h} $^1A_{1g}$)
0.0
[0.0]
{0.02}

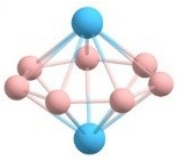

(C_{2v} $^3B_1$)
0.9
[1.5]
{0.02}

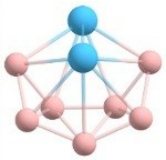

(C_s $^1A'$)
39.4
[38.9]
{0.05}

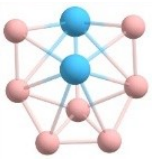

(C_1 ^1A)
41.1
[41.8]
{0.03}

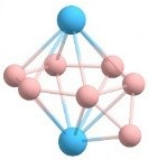

(C_s $^1A'$)
43.1
[50.1]
{0.04}

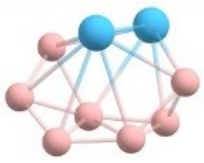

(C_1 ^1A)
43.1
[43.3]
{0.04}

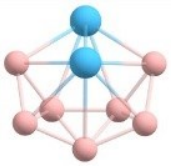

(C_1 ^3A)
46.5
[39.0]
{0.07}

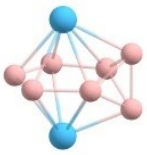

(C_{2v} $^1A_1$)
47.7
[48.3]
{0.04}

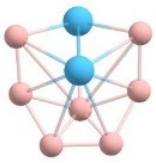

(C_s $^3A''$)
48.7
[48.7]
{0.04}

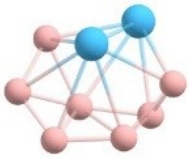

(C_1 ^3A)
50.8
[43.5]
{0.06}

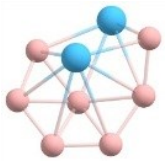

(C_1 ^3A)
53.4
[47.1]
{0.06}

Figure S2. Optimized structures of $B_7Hf_2^-$ at the PBE0/Def2-TZVPP level. The relative energy in kcal/mol computed at the single-point CCSD(T)/Def2-TZVPP//PBE0/Def2-TZVPP and PBE0/Def2-TZVPP (in square brackets) level with zero-point corrections of PBE0/Def2-TZVPP. T1 diagnostic, point group and spectroscopic states were given in curly brace and parenthesis, respectively.

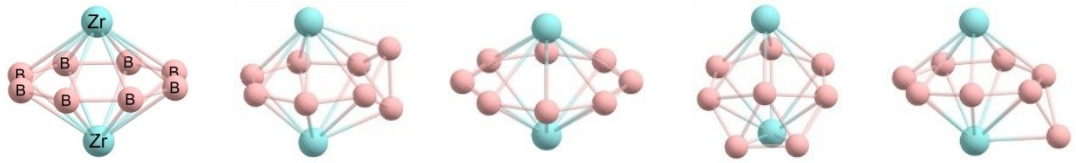

(D_{8h} $^1A_{1g}$) (C_{2v} $^1A_1$) (D_{2h} $^3B_{3u}$) (C_s $^1A'$) (C_1 ^3A)

0.0 14.8 27.4 34.7 45.7

[0.0] [7.1] [21.4] [26.7] [37.6]

{0.02} {0.03} {0.05} {0.03} {0.05}

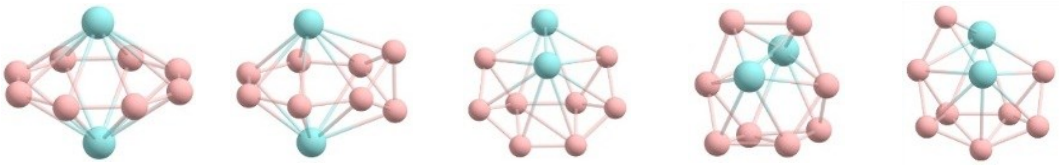

(D_{4h} $^3B_{2g}$) (C_{2v} $^3B_1$) (C_1 ^1A) (C_2 ^3A) (C_1 ^1A)

47.2 48.0 48.9 58.3 61.0

[32.4] [39.8] [40.9] [48.4] [52.5]

{0.03} {0.04} {0.05} {0.04} {0.04}

Figure S3. Optimized structures of B_8Zr_2 at the PBE0/Def2-TZVPP level. The relative energy in kcal/mol computed at the single-point CCSD(T)/Def2-TZVPP//PBE0/Def2-TZVPP and PBE0/Def2-TZVPP (in square brackets) level with zero-point corrections of PBE0/Def2-TZVPP. T1 diagnostic, point group and spectroscopic states were given in curly brace and parenthesis, respectively.

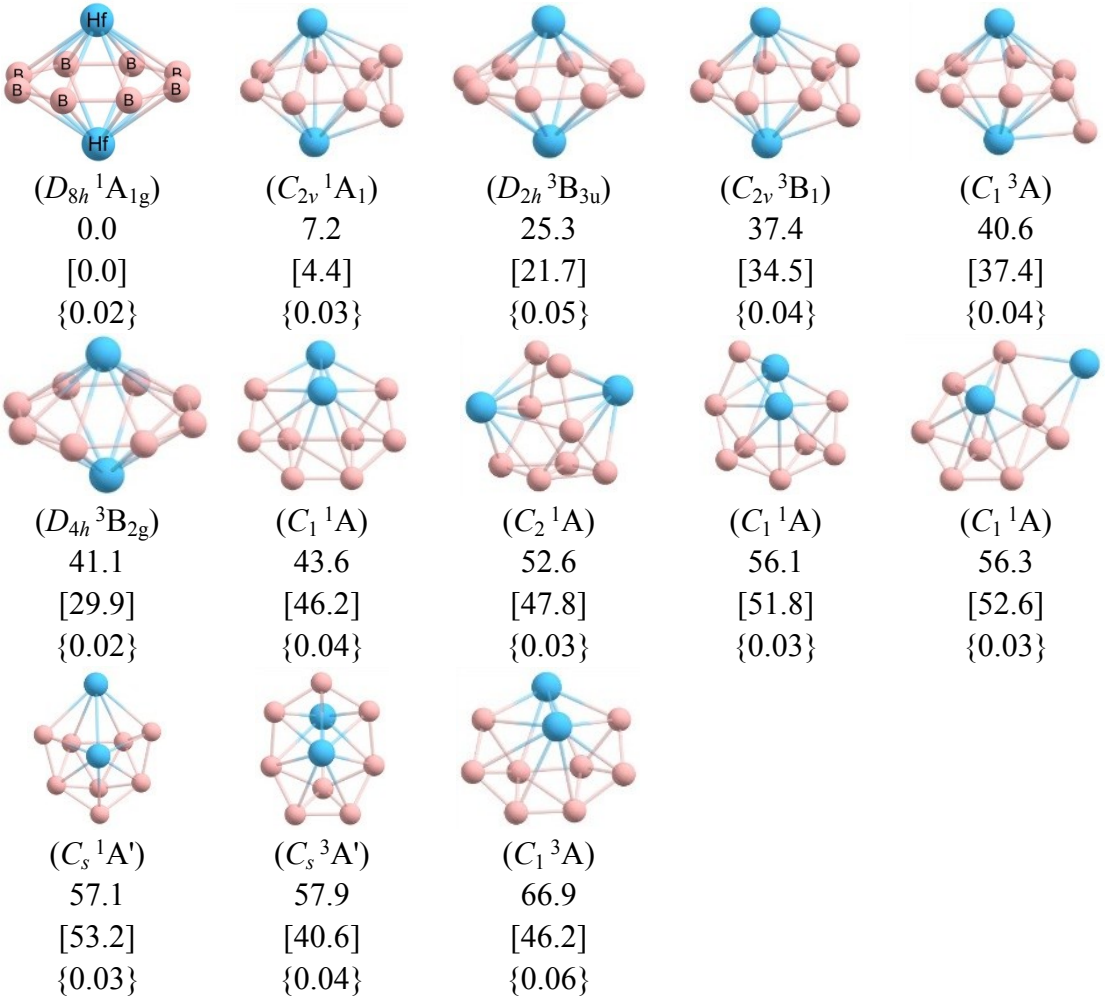

Figure S4. Optimized structures of B_8Hf_2 at the PBE0/Def2-TZVPP level. The relative energy in kcal/mol computed at the single-point CCSD(T)/Def2-TZVPP//PBE0/Def2-TZVPP and PBE0/Def2-TZVPP (in square brackets) level with zero-point corrections of PBE0/Def2-TZVPP. T1 diagnostic, point group and spectroscopic states were given in curly brace and parenthesis, respectively.

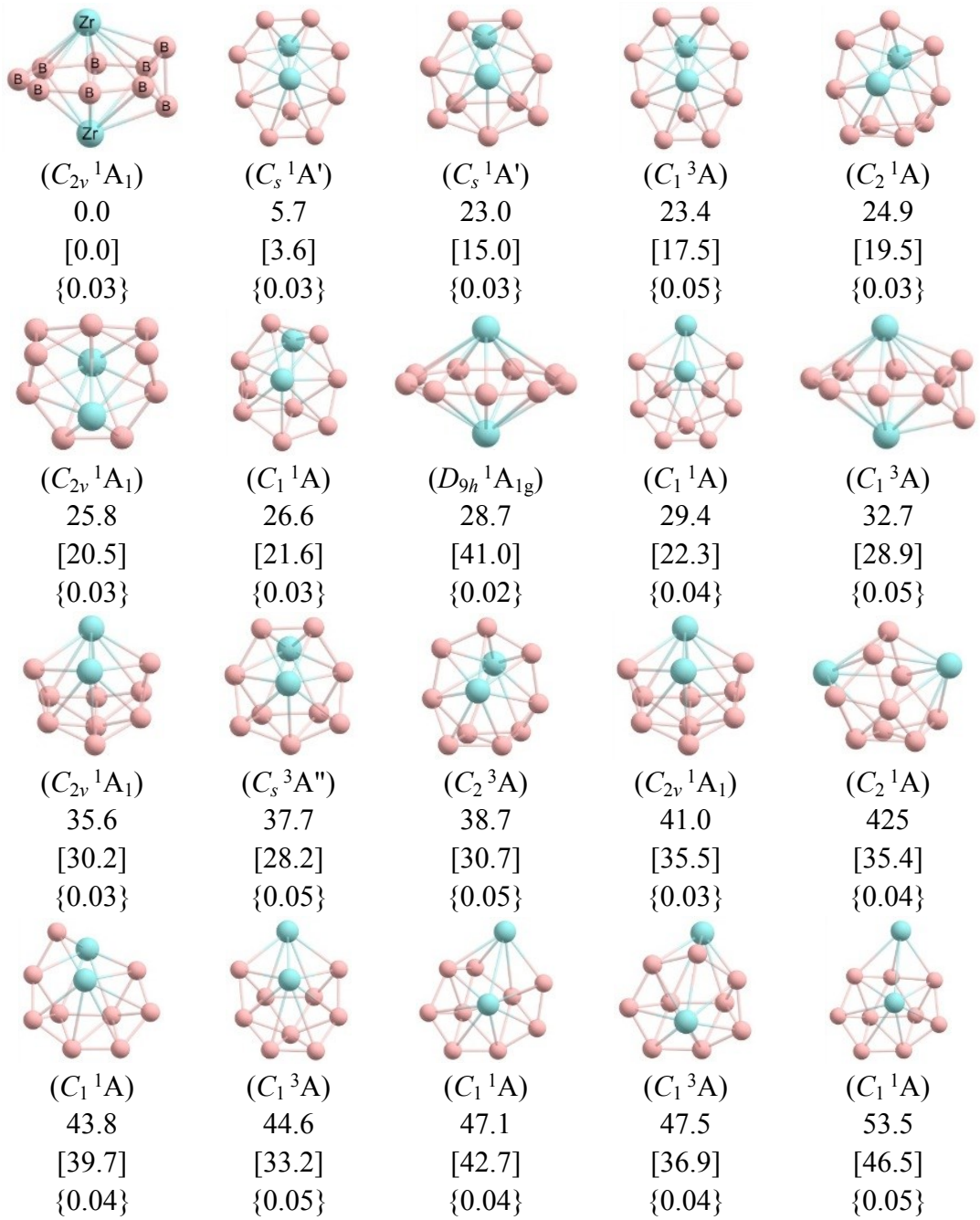

Figure S5. Optimized structures of $B_9Zr_2^+$ at the PBE0/Def2-TZVPP level. The relative energy in kcal/mol computed at the single-point CCSD(T)/Def2-TZVPP//PBE0/Def2-TZVPP and PBE0/Def2-TZVPP (in square brackets) level with zero-point corrections of PBE0/Def2-TZVPP. T1 diagnostic, point group and spectroscopic states were given in curly brace and parenthesis, respectively.

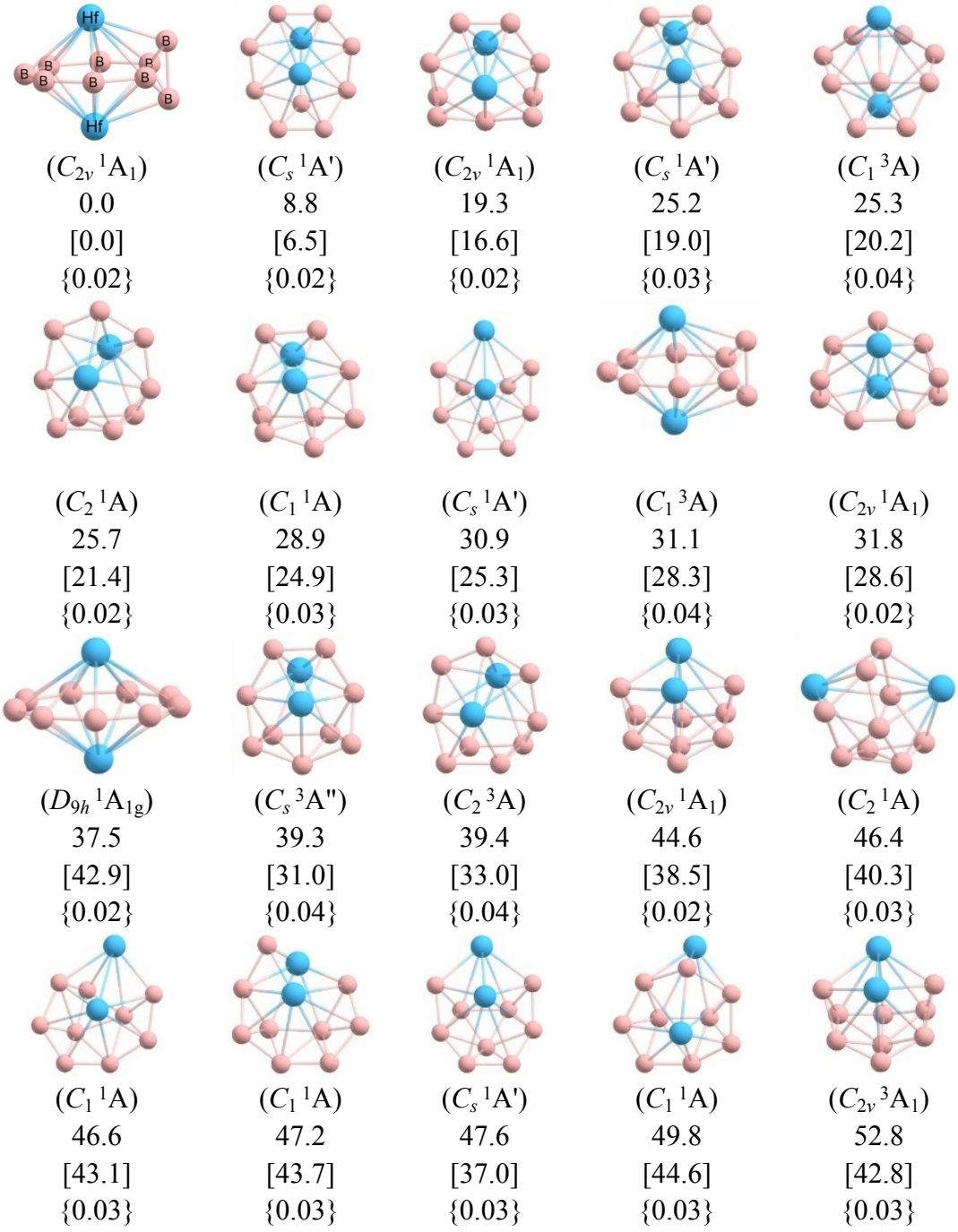

Figure S6. Optimized structures of $B_9Hf_2^+$ at the PBE0/Def2-TZVPP level. The relative energy in kcal/mol computed at the single-point CCSD(T)/Def2-TZVPP//PBE0/Def2-TZVPP and PBE0/Def2-TZVPP (in square brackets) level with zero-point corrections of PBE0/Def2-TZVPP. T1 diagnostic, point group and spectroscopic states were given in curly brace and parenthesis, respectively.

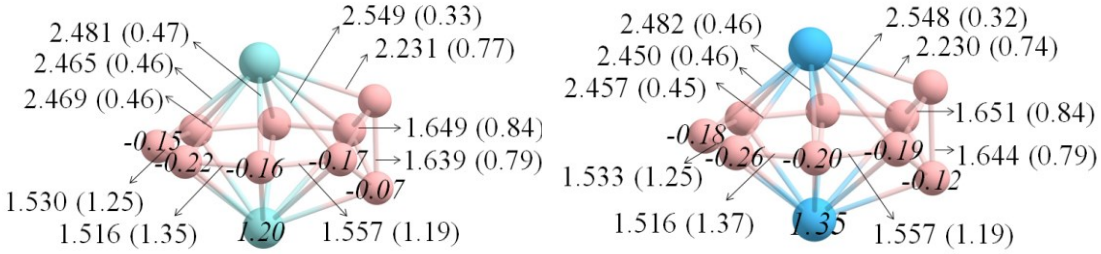

$B_9Zr_2^+$ $B_9Hf_2^+$

Figure S7. The structural properties of the C_{2v}-symmetry global $B_9M_2^+$ computed at the PBE0/Def2-TZVPP level. WBI and NPA charges is given in parenthesis and in italic.

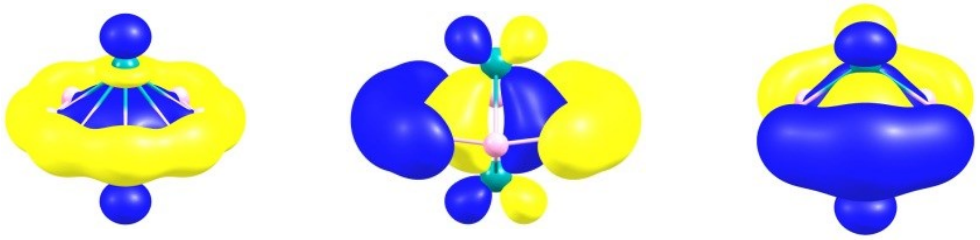

$B_7Hf_2^-$	16.9%	9.3%	9.3%
B_8Hf_2	15.5%	23.8%	23.8%
$B_9Hf_2^+$	12.7%	31.0%	31.0%
	Orb-25 (d_p-σ)	Orb-27 (d_p-σ)	Orb-28 (d_p-σ)

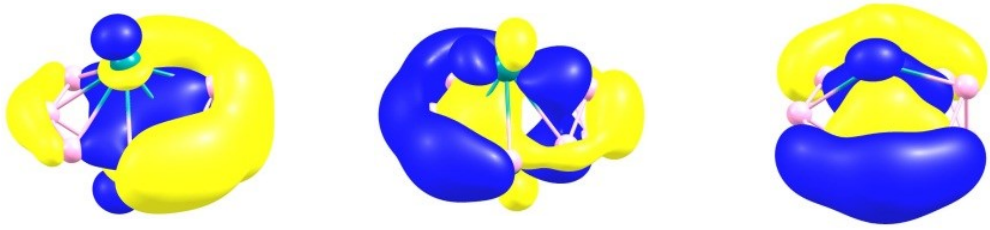

C_{2v}-$B_9Hf_2^+$	8.5%	20.5%	22.8%
	Orb-26 (d_p-σ)	Orb-30 (d_p-σ)	Orb-31 (d_p-σ)

Figure S8. The d_p-σ molecular orbitals of the D_{nh}-symmetry $B_7Hf_2^-$, B_8Hf_2, and $B_9Hf_2^+$ and C_{2v}-symmetry $B_9Hf_2^+$, where the proportion of the d orbitals of M_2 dimer is given in percentage.

Table S1. EDA-NOCV results of B_8Zr_2 in different electronic states (S: singlet, T: triplet) at the PBE0/TZ2P+ level of theory. Energy values are given in kcal/mol.

	B_8Zr_2				
fragments	B_8^{8-}(S) + Zr_2^{8+}(S)	B_8^{4-}(S) + Zr_2^{4+}(S)	B_8^{2-} (S) + Zr_2^{2+}(S)	B_8^{2-} (T) + Zr_2^{2+} (T)	B_8^{0} (S) + Zr_2^{0} (S)
ΔE_{int}	-8050.7	-2689.9	-1204.0	-1176.2	-853.8
ΔE_{disp}	-1.9	-5.6	-5.6	-5.6	-5.6
ΔE_{Pauli}	682.7	755.5	598.5	675.4	1002.1
ΔE_{elstat}[a]	*-6410.6*	*-1950.7*	*-775.8*	*-761.6*	*-652.7*
ΔE_{orb}[a]	*-2320.9*	*-1489.3*	*-1021.2*	*-1084.5*	*-1197.7*

[a]The values in parentheses give the percentage contribution to the total attractive interactions $\Delta E_{elstat} + \Delta E_{orb}$.

[b]The values in parentheses give the percentage contribution to the total orbital interactions ΔE_{orb}.

Table S2. EDA-NOCV results of the different charges of B_8Hf_2 at the PBE0/TZ2P+ level of theory. Energy values are given in kcal/mol.

	B_8Hf_2				
fragments	B_8^{8-}(S) + Hf_2^{8+}(S)	B_8^{4-}(S) + Hf_2^{4+}(S)	B_8^{2-} (S) + Hf_2^{2+}(S)	B_8^{2-} (T) + Hf_2^{2+} (T)	B_8^{0} (S) + Hf_2^{0} (S)
ΔE_{int}	-8077.9	-2536.1	-1127.7	-1212.5	-892.0
ΔE_{disp}	-4.2	-4.2	-4.2	-4.2	-4.2
ΔE_{Pauli}	717.4	892.1	927.8	720.0	1039.4
ΔE_{elstat}[a]	-6480.2	-1997.4	-1001.5	-865.0	-708.2
ΔE_{orb}[a]	*-2314.0*	*-1426.6*	*-1049.9*	*-1063.4*	*-1219.1*

[a]The values in parentheses give the percentage contribution to the total attractive interactions $\Delta E_{elstat} + \Delta E_{orb}$.

[b]The values in parentheses give the percentage contribution to the total orbital interactions ΔE_{orb}.

Figure S9. Plot of deformation densities Δρ of the pairwise orbital interactions and the associated interaction energies (ΔE_{orb}) between fragments in B_8Hf_2 (B_8^{2-} + Hf_2^{2+}). The direction of the charge flow is red to blue.

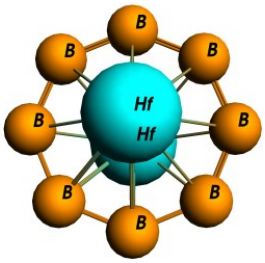

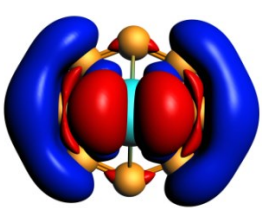

$\Delta E_{\rho 1\text{-}1}$ = -192.3 kcal/mol, $\nu_{1\text{-}1}$ = ±1.42

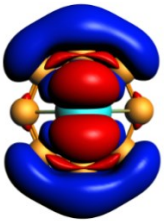

$\Delta E_{\rho 1\text{-}2}$ = -189.0 kcal/mol, $\nu_{1\text{-}2}$ = ±1.41

$\Delta E_{\rho 1}$ = -381.3 kcal/mol, ν_1 = ±2.83

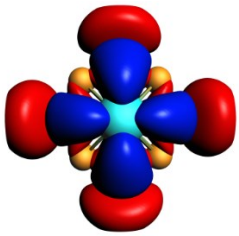

$\Delta E_{\rho 2\text{-}1}$ = -157.7 kcal/mol, $\nu_{2\text{-}1}$ = ±1.93

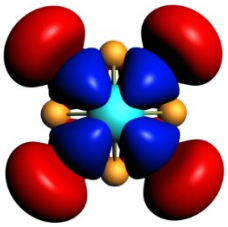

$\Delta E_{\rho 2\text{-}2}$ = -156.7 kcal/mol, $\nu_{2\text{-}2}$ = ±1.92

$\Delta E_{\rho 2}$ = -314.4 kcal/mol, ν_2 = ±3.85

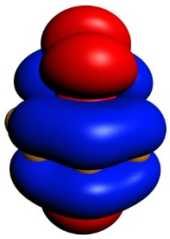

$\Delta E_{\rho 3\text{-}1}$ = -198.3 kcal/mol, $\nu_{3\text{-}1}$ = ±1.90

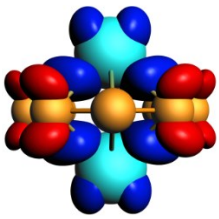

$\Delta E_{\rho 3\text{-}2}$ = -23.4 kcal/mol, $\nu_{3\text{-}2}$ = ±0.64

$\Delta E_{\rho 3}$ = -221.7 kcal/mol, ν_3 = ±2.54

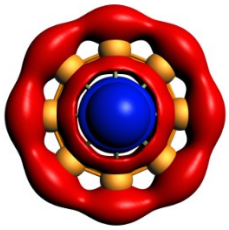

$\Delta E_{\rho 4}$ = -38.2 kcal/mol, ν_4 = ±0.95

Figure S10. Shape of the most important interacting MOs of fragments in B_8Hf_2 (B_8^{2-} + Hf_2^{2+}), plot of deformation densities Δρ of the pairwise orbital interactions and the associated interaction energies (ΔE_{orb}) between fragments. The direction of the charge flow is red to blue.

deformation densities Δρ	interacting MOs		
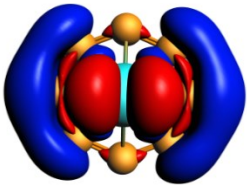 $\Delta E_{\rho 1\text{-}1}$ = -192.3 kcal/mol, $\nu_{1\text{-}1}$ = ±1.42	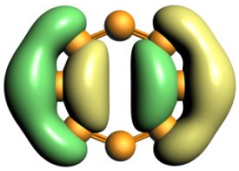 fra g1-6B2(LUMO+1) ν=1.284	←	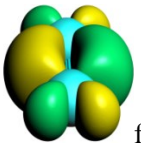 frag2-17B2(HOMO-1) ν = -1.202
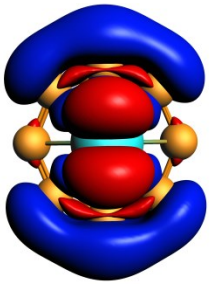 $\Delta E_{\rho 1\text{-}2}$ = -189.0 kcal/mol, $\nu_{1\text{-}2}$ = ±1.41	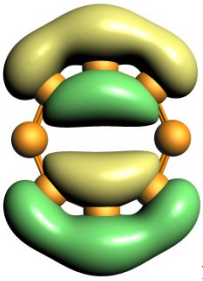 frag1-6B1(LUMO+2) ν = 1.272	←	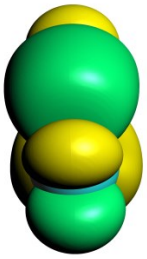 frag2-17B1(HOMO-2) ν = -1.202
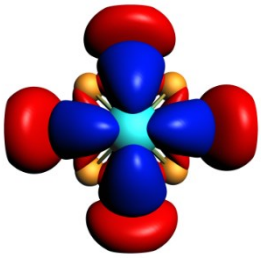 $\Delta E_{\rho 2\text{-}1}$ = -157.7 kcal/mol, $\nu_{2\text{-}1}$ = ±1.93	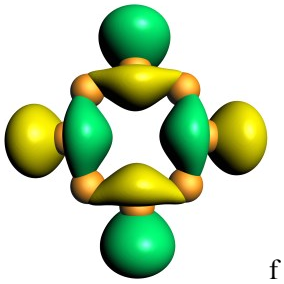 f rag1-8A1(HOMO-1) ν = -1.886	→	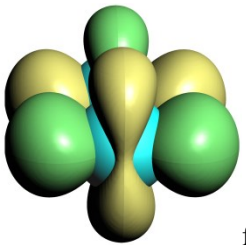 fra g2-34A1(LUMO+4) ν = 1.065
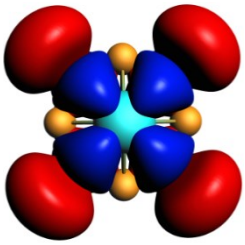 $\Delta E_{\rho 2\text{-}2}$ = -156.7 kcal/mol, $\nu_{2\text{-}2}$ = ±1.92	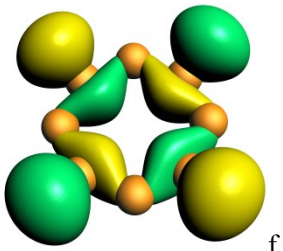 f rag1-4A2(HOMO) ν = -1.871	→	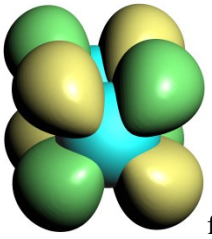 frag2-8A2(LUMO+5) ν = 1.113

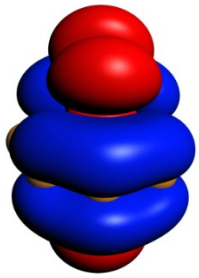 $\Delta E_{\rho 3\text{-}1}$ = -198.3 kcal/mol, $\nu_{3\text{-}1}$ = ±1.90	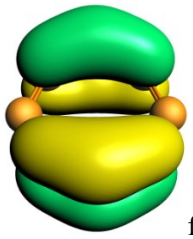 frag1-5B2(LUMO) ν = 1.529		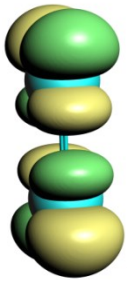 frag2-18B2(HOMO) ν = -1.834
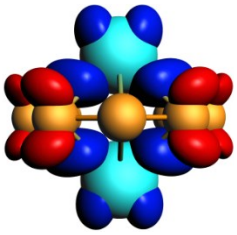 $\Delta E_{\rho 3\text{-}2}$ = -23.4 kcal/mol, $\nu_{3\text{-}2}$ = ±0.64	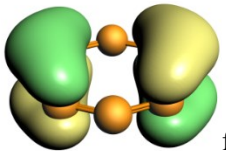 frag1-5B1(HOMO-2) ν = -0.476		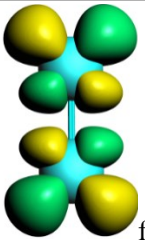 frag2-18B1(LUMO+6) ν = 0.188
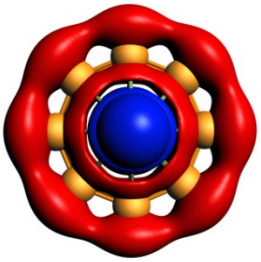 $\Delta E_{\rho 4}$ = -38.2 kcal/mol, ν_4 = ±0.95	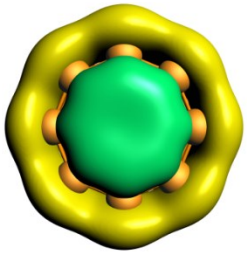 frag1-6A1(HOMO-4) ν = -0.705		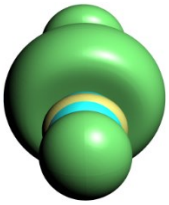 frag2-31A1(LUMO) ν = 0.630
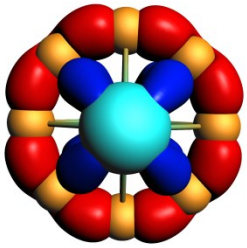 $\Delta E_{\rho 5\text{-}1}$ = -18.5 kcal/mol, $\nu_{5\text{-}1}$ = ±0.40	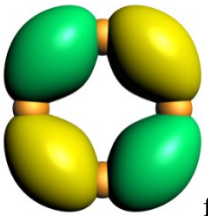 frag1-2A2(HOMO-9) ν = -0.274		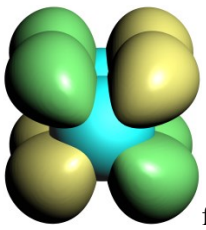 frag2-7A2(LUMO+2) ν = 0.247
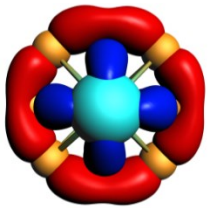 $\Delta E_{\rho 5\text{-}2}$ = -18.4 kcal/mol, $\nu_{5\text{-}2}$ = ±0.40	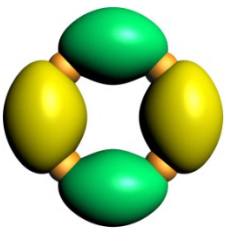 frag1-5A1(HOMO-8) ν = -0.272		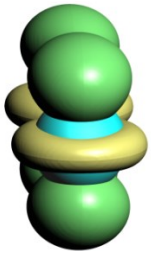 frag2-32A1 (LUMO+1) ν = 0.174

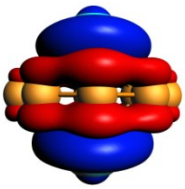 $\Delta E_{\rho 6}$ = -20.1 kcal/mol, $\nu_6 = \pm 0.48$	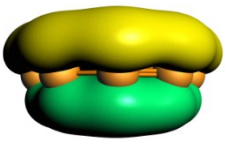 frag 1-7A1(HOMO-3) ν = -0.614		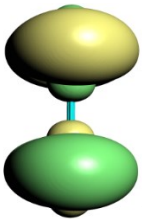 frag2-35A1(LUMO+7) ν = 0.630

Figure S11. Plot of deformation densities Δρ of the pairwise orbital interactions and the associated interaction energies (ΔE_{orb}) between fragments in B_8Zr_2 (B_8^{2-} + Zr_2^{2+}). The direction of the charge flow is red to blue.

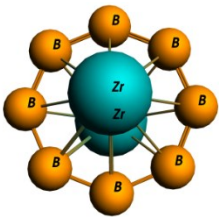

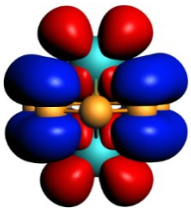

$\Delta E_{\rho 1\text{-}1}$ = -194.8 kcal/mol, $\nu_{1\text{-}1}$ = ±1.86

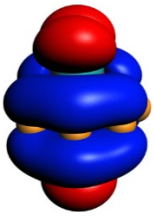

$\Delta E_{\rho 1\text{-}2}$ = -190.0 kcal/mol, $\nu_{1\text{-}2}$ = ±1.85

$\Delta E_{\rho 1}$ = -384.8 kcal/mol, ν_1 = ±3.71

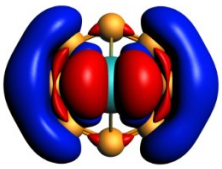

$\Delta E_{\rho 2\text{-}1}$ = -204.6 kcal/mol, $\nu_{2\text{-}1}$ = ±1.46

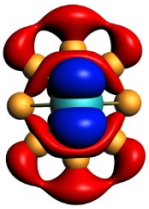

$\Delta E_{\rho 2\text{-}2}$ = -69.5 kcal/mol, $\nu_{2\text{-}2}$ = ±0.97

$\Delta E_{\rho 2}$ = -274.1 kcal/mol, ν_2 = ±2.43

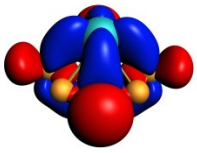

$\Delta E_{\rho 3}$ = -156.0 kcal/mol, ν_3 = ±1.94

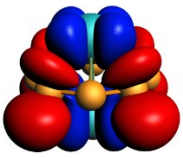

$\Delta E_{\rho 4}$ = -99.1 kcal/mol, ν_4 = ±1.25

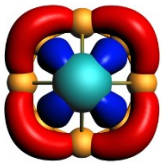

$\Delta E_{\rho 5\text{-}1}$ = -22.9 kcal/mol, $\nu_{5\text{-}1}$ = ±0.43

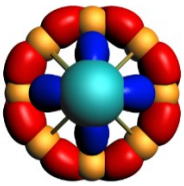

$\Delta E_{\rho 5\text{-}2}$ = -16.3 kcal/mol, $\nu_{5\text{-}2}$ = ±0.39

$\Delta E_{\rho 5}$ = -39.2 kcal/mol, ν_5 = ±0.82

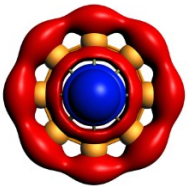

$\Delta E_{\rho 6}$ = -36.1 kcal/mol, ν_6 = ±0.94

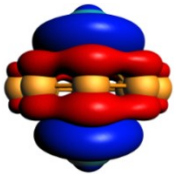

$\Delta E_{\rho 7}$ = -17.7 kcal/mol, ν_7 = ±0.48

Figure S12. Shape of the most important interacting MOs of fragments in B_8Zr_2 (B_8^{2-} + Zr_2^{2+}), plot of deformation densities Δρ of the pairwise orbital interactions and the associated interaction energies (ΔE_{orb}) between fragments. The direction of the charge flow is red to blue.

deformation densities Δρ	interacting MOs		
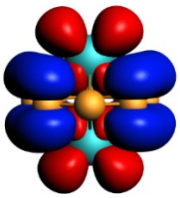 $\Delta E_{\rho 1\text{-}1}$ = -194.8 kcal/mol, $\nu_{1\text{-}1}$ = ±1.86	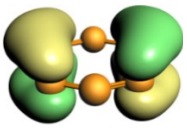 frag1-5B2(LUMO) ν = 1.501		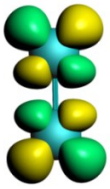 frag2-10B2(HOMO-1) ν = -1.773
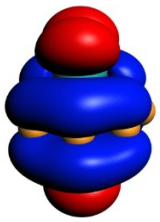 $\Delta E_{\rho 1\text{-}2}$ = -190.0 kcal/mol, $\nu_{1\text{-}2}$ = ±1.85	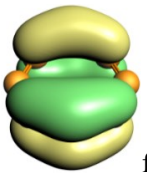 frag1-5B1(LUMO+2) ν = 1.495		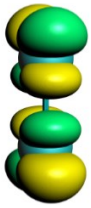 frag2-10B1(HOMO-2) ν = -1.771
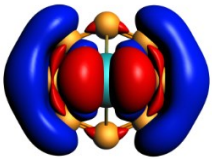 $\Delta E_{\rho 2\text{-}1}$ = -204.6 kcal/mol, $\nu_{2\text{-}1}$ = ±1.46	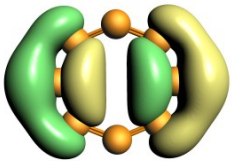 frag1-6B2(LUMO+1) ν = 1.304		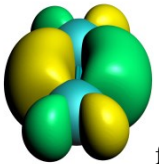 frag2-9B2(HOMO-3) ν = -1.293
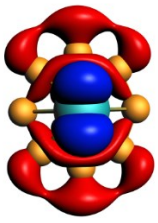 $\Delta E_{\rho 2\text{-}2}$ = -69.5 kcal/mol, $\nu_{2\text{-}2}$ = ±0.97	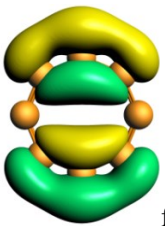 frag1-6B1(HOMO-2) ν = -0.702		 frag2-9B1(LUMO+1) ν = 0.701
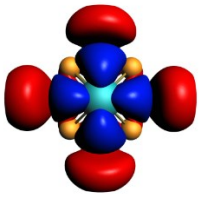 $\Delta E_{\rho 3}$ = -156.0 kcal/mol, ν_3 = ±1.94	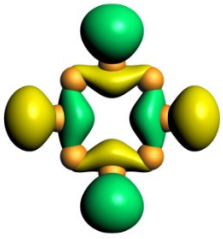 frag1-8A1(HOMO-1) ν = -1.898		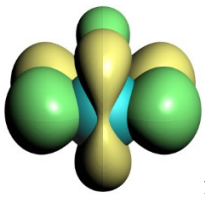 frag2-22A1(LUMO+4) ν = 1.077

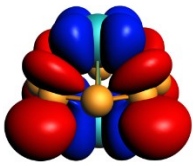 $\Delta E_{\rho 4}$ = -99.1 kcal/mol, ν_4 = ±1.25	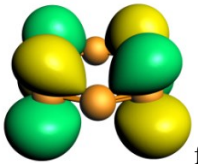 frag1- 4A2(HOMO) ν = -1.213	—	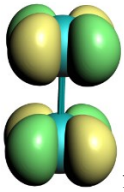 frag2- 4A2(LUMO+4) ν = 1.132
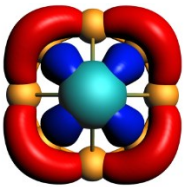 $\Delta E_{\rho 5\text{-}1}$ = -22.9 kcal/mol, $\nu_{5\text{-}1}$ = ±0.43	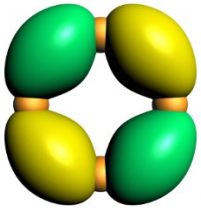 frag1- 2A2(HOMO-8) ν = -0.236	—	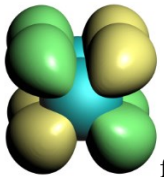 frag2- 3A2(LUMO+3) ν = 0.212
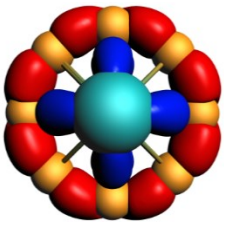 $\Delta E_{\rho 5\text{-}2}$ = -16.3 kcal/mol, $\nu_{5\text{-}2}$ = ±0.39	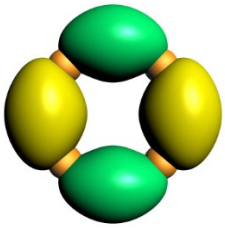 frag 1-5A1(HOMO-8) ν = -0.219	—	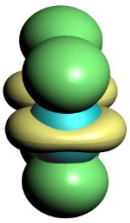 frag2- 20A1(LUMO+2) ν = 0.158
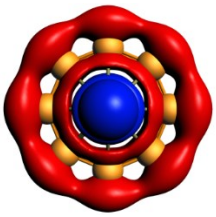 $\Delta E_{\rho 6}$ = -36.1 kcal/mol, ν_6 = ±0.94	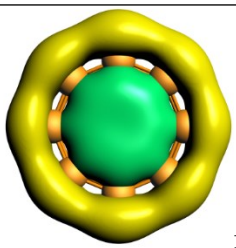 fra g1-7A1(HOMO-3) ν = -0.766	—	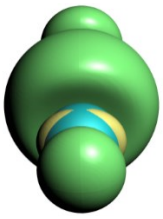 frag2- 19A1 (LUMO) ν = 0.729
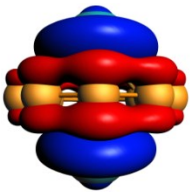 $\Delta E_{\rho 7}$ = -17.7 kcal/mol, ν_7 = ±0.48	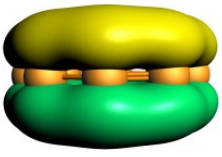 frag 1-6A1(HOMO-4) ν = -0.633	—	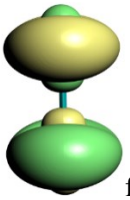 frag2- 23A1(LUMO+6) ν = 0.567

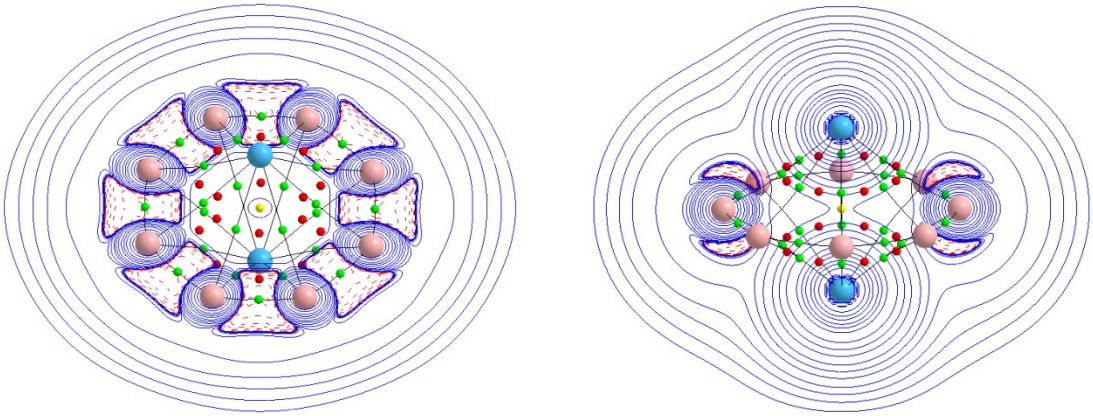

(a) (b)

Figure S13. Laplacian distribution of B_8Zr_2 at the PBE0/Def2-TZVPP level. (a): The plane of the B_8 ring. (b): The plane that contains the Zr atoms and two opposing B atoms bisecting the plane of the B_8 ring. Red lines indicate areas of charge concentration ($\nabla^2\rho(r) < 0$) while blue lines show areas of charge depletion ($\nabla^2\rho(r) > 0$). The solid lines connecting the atomic nuclei are the bond paths. Green dots are bond critical points, red dots are ring critical points, and the two yellow dots are the cage critical points.

Table S3. Coordinates of D_{nh}-symmetry minimum

$B_7Zr_2^-$

E_{PBE0} = -267.823032

E_{ZPE} = 0.030606

B	0.000000	1.801476	0.000000
B	-1.408451	1.123202	0.000000
B	-0.781631	-1.623074	0.000000
B	0.781631	-1.623074	0.000000
B	1.756309	-0.400866	0.000000
B	1.408451	1.123202	0.000000
B	-1.756309	-0.400866	0.000000
Zr	0.000000	0.000000	1.523881
Zr	0.000000	0.000000	-1.523881

$B_7Hf_2^-$

E_{PBE0} = -269.708362

E_{ZPE} = 0.02989

B	0.000000	1.808534	0.000000
B	-1.413969	1.127602	0.000000
B	-0.784693	-1.629433	0.000000
B	0.784693	-1.629433	0.000000
B	1.763190	-0.402437	0.000000
B	1.413969	1.127602	0.000000
B	-1.763190	-0.402437	0.000000
Hf	0.000000	0.000000	1.502414
Hf	0.000000	0.000000	-1.502414

B_8Zr_2

E_{PBE0} = -292.600299

E_{ZPE} = 0.035008

B	0.000000	1.988702	0.000000
B	-1.988702	0.000000	0.000000
B	-1.406225	1.406225	0.000000
B	1.988702	0.000000	0.000000
B	1.406225	1.406225	0.000000
B	-1.406225	-1.406225	0.000000
B	0.000000	-1.988702	0.000000
B	1.406225	-1.406225	0.000000
Zr	0.000000	0.000000	1.469584
Zr	0.000000	0.000000	-1.469584

B_8Hf_2

E_{PBE0} = -294.493404

E_{ZPE} = 0.034598

B	0.000000	1.993785	0.000000
B	-1.993785	0.000000	0.000000
B	-1.409819	1.409819	0.000000
B	1.993785	0.000000	0.000000
B	1.409819	1.409819	0.000000
B	-1.409819	-1.409819	0.000000
B	0.000000	-1.993785	0.000000
B	1.409819	-1.409819	0.000000
Hf	0.000000	0.000000	1.445399
Hf	0.000000	0.000000	-1.445399

$B_9Zr_2^+$

E_{PBE0} = -317.1286819

E_{ZPE} = 0.036534

B	0.000000	2.194442	0.000000
B	-0.750543	-2.062101	0.000000
B	-2.161103	0.381061	0.000000
B	2.161103	0.381061	0.000000
B	-1.900442	-1.097221	0.000000
B	1.410560	1.681040	0.000000
B	0.750543	-2.062101	0.000000
B	-1.410560	1.681040	0.000000
B	1.900442	-1.097221	0.000000
Zr	0.000000	0.000000	1.444766
Zr	0.000000	0.000000	-1.444766

$B_9Hf_2^+$

E_{PBE0} = -319.026390

E_{ZPE} = 0.036278

B	0.000000	2.197258	0.000000
B	-0.751506	-2.064747	0.000000
B	-2.163876	0.381550	0.000000
B	2.163876	0.381550	0.000000
B	-1.902881	-1.098629	0.000000
B	1.412370	1.683197	0.000000
B	0.751506	-2.064747	0.000000
B	-1.412370	1.683197	0.000000
B	1.902881	-1.098629	0.000000
Hf	0.000000	0.000000	1.420456
Hf	0.000000	0.000000	-1.420456

Table S4. Coordinates of C_{2v}-ymmetry minimum

$B_7Zr_2^-$
E_{PBE0} = -267.736763
E_{ZPE} = 0.02907

B	0.000000	0.809488	-1.818698
B	0.000000	-0.809488	-1.818698
B	1.210343	0.000000	-0.885614
B	-1.210343	0.000000	-0.885614
B	0.000000	0.000000	1.528563
B	1.416841	0.000000	0.735970
B	-1.416841	0.000000	0.735970
Zr	0.000000	-1.721970	0.150508
Zr	0.000000	1.721970	0.150508

$B_7Hf_2^-$
E_{PBE0} = -269.629905
E_{ZPE} = 0.028382

B	0.000000	0.815947	-1.875820
B	0.000000	-0.815947	-1.875820
B	1.205249	0.000000	-0.928262
B	-1.205249	0.000000	-0.928262
B	0.000000	0.000000	1.480665
B	1.419238	0.000000	0.696245
B	-1.419238	0.000000	0.696245
Hf	0.000000	-1.719874	0.094966
Hf	0.000000	1.719874	0.094966

B_8Zr_2
E_{PBE0} = -292.589603
E_{ZPE} = 0.035570

B	0.000000	1.286868	1.163402
B	0.000000	1.719656	-0.361367
B	0.000000	0.786116	-1.602673
B	0.000000	-1.719656	-0.361367
B	-0.808065	0.000000	1.892417
B	0.808065	0.000000	1.892417
B	0.000000	-0.786116	-1.602673
B	0.000000	-1.286868	1.163402
Zr	-1.622159	0.000000	-0.136472
Zr	1.622159	0.000000	-0.136472

B_8Hf_2
E_{PBE0} = -294.486911

E_{ZPE} = 0.035068

B	0.000000	1.726604	-0.312166
B	0.000000	-0.787639	-1.553339
B	0.000000	1.288582	1.211425
B	-0.810765	0.000000	1.943027
B	0.000000	-1.726604	-0.312166
B	0.810765	0.000000	1.943027
B	0.000000	0.787639	-1.553339
B	0.000000	-1.288582	1.211425
Hf	1.615121	0.000000	-0.089510
Hf	-1.615121	0.000000	-0.089510

$B_9Zr_2^+$

E_{PBE0} = -317.197598

E_{ZPE} = 0.040063

B	0.000000	1.933492	0.008148
B	0.000000	1.313327	-1.419553
B	0.000000	-1.404566	1.428871
B	-0.819628	0.000000	-1.987924
B	0.000000	-1.933492	0.008148
B	0.000000	-1.313327	-1.419553
B	0.000000	0.000000	2.035287
B	0.819628	0.000000	-1.987924
B	0.000000	1.404566	1.428871
Zr	-1.551625	0.000000	0.119102
Zr	1.551625	0.000000	0.119102

$B_9Hf_2^+$

E_{PBE0} = -319.098124

E_{ZPE} = 0.039671

B	0.000000	1.942596	-0.039896
B	0.000000	1.315826	-1.464889
B	0.000000	-1.407828	1.379017
B	-0.822082	0.000000	-2.030508
B	0.000000	-1.942596	-0.039896
B	0.000000	-1.315826	-1.464889
B	0.000000	0.000000	1.986201
B	0.822082	0.000000	-2.030508
B	0.000000	1.407828	1.379017
Hf	-1.540661	0.000000	0.080776
Hf	1.540661	0.000000	0.080776